

# Class I TCP transcription factor AtTCP8 modulates key brassinosteroid-responsive genes

Benjamin J. Spears ,<sup>1,2,3,\*</sup> Samuel A. McInturf,<sup>2,3</sup> Carina Collins ,<sup>4</sup> Meghann Chlebowski ,<sup>1</sup> Leland J. Cseke ,<sup>2,3</sup> Jianbin Su ,<sup>2,3</sup> David G. Mendoza-Cózatl<sup>2,3</sup> and Walter Gassmann ,<sup>2,3</sup>

<sup>1</sup> Department of Biological Sciences, Butler University, Indianapolis, Indiana, USA

<sup>2</sup> Division of Plant Science and Technology, University of Missouri, Columbia, Missouri, USA

<sup>3</sup> Christopher S. Bond Life Sciences Center and Interdisciplinary Plant Group, University of Missouri, Columbia, Missouri, USA

<sup>4</sup> Department of Biology, Marian University, Indianapolis, Indiana, USA

\*Author for correspondence: [bjspears1@butler.edu](mailto:bjspears1@butler.edu)

B.J.S. and W.G. planned and designed the research. B.J.S., M.C., C.C., and L.J.C. performed experiments. J.S. provided technical assistance and supervision to B.J.S. B.J.S., S.A.M., M.C., C.C., D.G.M.C., and W.G. analyzed and interpreted data. B.J.S. wrote the article with editing contributions from all of the other authors.

The author responsible for distribution of materials integral to the findings presented in this article in accordance with the policy described in the Instructions for Authors (<https://academic.oup.com/plphys/pages/general-instructions>) is B.J.S. ([bjspears1@butler.edu](mailto:bjspears1@butler.edu)).

## Abstract

The plant-specific TEOSINTE BRANCHED1/CYCLOIDEA/PROLIFERATING CELL FACTOR (TCP) transcription factor family is most closely associated with regulating plant developmental programs. Recently, TCPs were also shown to mediate host immune signaling, both as targets of pathogen virulence factors and as regulators of plant defense genes. However, comprehensive characterization of TCP gene targets is still lacking. Loss of function of the class I TCP gene AtTCP8 attenuates early immune signaling and, when combined with mutations in AtTCP14 and AtTCP15, additional layers of defense signaling in *Arabidopsis* (*Arabidopsis thaliana*). Here, we focus on TCP8, the most poorly characterized of the three to date. We used chromatin immunoprecipitation and RNA sequencing to identify TCP8-bound gene promoters and differentially regulated genes in the *tcp8* mutant; these datasets were heavily enriched in signaling components for multiple phytohormone pathways, including brassinosteroids (BRs), auxin, and jasmonic acid. Using BR signaling as a representative example, we showed that TCP8 directly binds and activates the promoters of the key BR transcriptional regulatory genes *BRASSINAZOLE-RESISTANT1* (*BZR1*) and *BRASSINAZOLE-RESISTANT2* (*BZR2/BES1*). Furthermore, *tcp8* mutant seedlings exhibited altered BR-responsive growth patterns and complementary reductions in *BZR2* transcript levels, while TCP8 protein demonstrated BR-responsive changes in subnuclear localization and transcriptional activity. We conclude that one explanation for the substantial targeting of TCP8 alongside other TCP family members by pathogen effectors may lie in its role as a modulator of BR and other plant hormone signaling pathways.

## Introduction

Plants must be able to perceive diverse local environmental conditions and integrate that data into an appropriate biological response. In addition to abiotic stresses like light, water, and nutrient availability, a successful plant must also be

able to respond to the presence of a variety of different pests and pathogens to protect itself from disease. The metabolic costs of these distinct biological processes mandate tight control to allow plants to respond appropriately to stresses without unnecessary costs to growth and development that

arise from unregulated signaling (Couto and Zipfel, 2016). These balances are largely governed through a complex network of phytohormone signaling pathways (Shigenaga et al., 2017). This tradeoff is exemplified by yield loss in crop species and the model plant *Arabidopsis* (*Arabidopsis thaliana*) conferred through enhanced immune signaling (Ning et al., 2017). Even more striking is the severe growth inhibition observed in *Arabidopsis* plants continuously exposed to immune elicitors, or mutants constitutively expressing defense genes (van Wersch et al., 2016). It is likely not only the intensity of either signaling pathway, but rather the tactical precision with which they are activated that may determine the success of a plant. Small perturbations in phytohormone status can therefore dramatically influence a plant's ability to defend itself, its growth potential, or both. This is a principle that pathogens have evolved to exploit to their benefit through the secretion of host-modulating virulence factors (Ma and Ma, 2016).

The plant immune system is a multilayered signaling network that offers robust protection against infection by most pathogens. Plants deploy a suite of pattern recognition receptors, among them the leucine-rich repeat receptor-like kinases (LRR-RLKs) FLS2 and EFR, to the cell surface that interact with specific sets of pathogen or microbe-associated molecular patterns (PAMPs and MAMPs) (Macho and Zipfel, 2014). Upon detection of a potential extracellular threat, LRR-RLKs transmit the signal to the cell interior through their kinase domains, activating a signal transduction cascade that extends to the nucleus. There the activities of transcriptional regulators are altered, likely through corresponding changes in protein modifications, stability, interactions, and localization, to modulate gene expression toward the production of diverse physiological responses, ultimately restricting pathogen virulence and growth. This collective response is known as PAMP-triggered immunity (PTI). PTI is thought to be antagonized by the signaling pathways of hormones such as brassinosteroids (BRs), as a part of the well-established tradeoff. This occurs potentially at the level of signal perception through the shared LRR-RLK BAK1 and associated regulators, at the level of reactive oxygen species (ROS) production or other signal propagations, or through other downstream responses including immunity and BR-related transcription factor (TF) activities (Albrecht et al., 2012; Belkhadir et al., 2012; Lin et al., 2013; Lozano-Duran et al., 2013). While these individual branches of the immune signaling response may be modulated in different directions by different environmental factors, their "net sum" after influence of hormone perception contributes to overall pathogen resistance or susceptibility (Smith et al., 2014). Further, inactivation of the immune response through targeting and disabling of critical signaling components by secreted effector proteins, often altering phytohormone balances, is a major strategy by which plant pathogens promote virulence (Zhou et al., 2014; Ahmed et al., 2018; Ceulemans et al., 2021).

Immune signaling has only recently been folded into the transcriptional repertoire of the 24-member TEOSINTE BRANCHED1/CYCLOIDEA/PROLIFERATING CELL FACTOR (TCP) TF family in *Arabidopsis*, but regulation is evident at multiple levels (Kim et al., 2014; Yang et al., 2017; Li et al., 2018; Zhang et al., 2018; Spears et al., 2019). TCPs have largely been characterized as regulators of many facets of plant growth and development in a semi-redundant fashion, among others cell elongation and proliferation, stature, germination, flowering time, pollen development, and leaf morphology (Li, 2015). In support of these diverse developmental roles, TCPs have also been implicated in the direct regulation of both biosynthesis and signaling pathways of many plant hormones, including jasmonic acid (JA), salicylic acid (SA), cytokinin (CK), ABA, auxin, and BR (Schommer et al., 2008; Guo et al., 2010; Mukhopadhyay and Tyagi, 2015; Wang et al., 2015; Gonzalez-Grandio et al., 2017). TCP family members are separated into two classes (I/II) based on the structure of their conserved DNA binding and dimerization domains. Within a class, individual TCP activities are generally additive while inter-class functions are reductive; however, exceptions to this organization are commonly observed (Nicolas and Cubas, 2016). As seen with related basic helix-loop-helix (bHLH) TFs like the PHYTOCHROME-INTERACTING FACTOR (PIF) and BZR families, heterodimeric interactions between TCPs of either class and with other TF families hints at a complex mechanism of regulation that often requires higher-order mutants to explore (Martínez and Sinha, 2013; Davière et al., 2014) and that may function to ensure the environmentally proper composition of plant hormone signaling (Danisman et al., 2013). It is fitting, then, that several TCPs of both classes have been identified as the targets of secreted effector proteins from multiple pathogens (Sugio et al., 2011; Weßling et al., 2014; Lopez et al., 2015; Yang et al., 2017; González-Fuente et al., 2020), potentially as part of an evolved strategy to promote virulence through modulation of these phytohormone signaling pathways.

Previous studies have described redundancies in regulation of host immunity by the trio of class I members TCP8, TCP14, and TCP15 (Kim et al., 2014; Li et al., 2018; Spears et al., 2019). However, recent work has pointed toward individual modes of action for each of these TCPs in the regulation of unique sets of defense and development-related phytohormone signaling components. TCP14 directly suppresses JA signaling (Yang et al., 2017) and TCP15 activates the transcription of PATHOGENESIS-RELATED5 (PR5) and SUPPRESSOR OF *npr1-1*, CONSTITUTIVE1 (SNC1) (Li et al., 2018; Zhang et al., 2018), and TCP8 the transcription of ISOCHORISMATE SYNTHASE1 (ICS1) (Wang et al., 2015) to promote SA signaling to the same effect. TCP15 and TCP14 are often implicated together in the control of CK and GA-dependent cell division and germination (Steiner et al., 2012; Lucero et al., 2015; Gastaldi et al., 2020), but TCP8 is generally uninvolved. Of the trio, TCP8 has been relatively

understudied particularly in the context of growth- and development-related functions.

Here, we aimed to further characterize the activities of TCP8 individually; to this end, we performed chromatin immunoprecipitation (ChIP-seq) and RNA-sequencing (RNA-seq) to identify patterns of genome-wide TCP8-bound promoters and differential gene expression between wild-type (WT), *tcp8* single, and *tcp8 tcp14 tcp15* triple (*t8t14t15*) mutants. We describe the enrichment of phytohormone signaling genes in multiple pathways and further validate our sequencing data by characterizing a previously undescribed role for TCP8 in contributing to the regulation of BR signaling. Our data show that TCP8 directly binds and transcriptionally activates key BR gene promoters in planta, that the activity and subcellular localization of TCP8 is BR-dependent, and through 24-epiBL (BL) insensitivity and brassinazole (Brz) hypersensitivity assays, that *tcp8* is compromised in BR signaling. Additionally, we demonstrate that TCP8 interacts directly with master BR regulators BZR1 and BZR2 in multiple expression systems, findings that support the notion of TCP heterodimerization with other TF families in a complex regulatory module to broadly regulate BR and other hormone signaling pathways in *Arabidopsis*.

## Results

### Differential regulation of hormone signaling pathways by class I TCPs

We generated a genome-wide profile of TCP8-interacting gene promoters to clarify mechanisms by which TCP8 is capable of regulating both defense and developmental signaling. ChIP-seq in a previously characterized native promoter-driven *pTCP8:TCP8-HA* [*t8t14t15*] transgenic line (Spears et al., 2019) was used to identify ~3,500 TCP8-binding sites across the genome (Supplemental Table S1). Although 16% of identified candidate peaks (568) were located within 3-kb upstream of an established TSS, most peaks were located in nonpromoter regions (Figure 1A; Supplemental Table S2). This is not an unusual feature of some TFs, especially in the bHLH family (Heyndrickx et al., 2014). For the purpose of our study, we focused on the subset of genes with promoter-localized binding sites.

From these candidate binding sites, we scanned the surrounding 500-bp regions for identification of enriched sequence motifs (Figure 1B). As expected, the most significantly enriched motif (GTGGGxCCAC) corresponds to a canonical class I TCP-binding site (O'Malley et al., 2016). Other notable motifs include the binding site for the immunity-suppressing CAMTA TF family (CGCGT), the GCC-box (GCCGCC) of AP2/EREBP factors that regulate ethylene and ABA signaling (Dietz et al., 2010), and the G-box (CACGTG) of PIF and BZR TF families, known for regulation of plant growth and response to environmental light conditions. Notably, genetic interactions between BZRs/PIFs and TCPs have been well-characterized (Perrella et al., 2018; Zhou et al., 2018, 2019; Ferrero et al., 2019).

Given the established role of TCP8 in the host immune response, the enrichment of SA-regulatory genes such as WRKY40 are unsurprising and highlight these candidates as potential causal factors for future study. For BR-related genes tested, including the regulatory TFs BEE3, BZR1, and BZR2, peaks corresponded to regions containing TCP-binding sites (Figure 1C). We have highlighted the largest peak heights and most notable pathway representative candidates of these categories (Table 1). A gene ontology (GO) term enrichment analysis identified significant enrichment of genes involved in BR signaling, as well as most major phytohormone signaling pathways, including strong enrichment of auxin-related genes (Figure 1D).

To further interrogate TCP8-specific signaling roles, we performed RNA-seq analysis comparing total mRNA collected from Col-0, *tcp8*, and *t8t14t15* seedlings under our ChIP-seq growth conditions to identify sets of genes for which differential expression was observed between Col-0 and *tcp8*, Col-0 and *t8t14t15*, or both. A total of 1,423 differentially expressed genes (DEGs) were identified in *tcp8* and 3,524 DEGs in *t8t14t15* (Figure 1E; Supplemental Table S3). These mutations had relatively low magnitude of effect overall on global gene expression, an observation that could possibly be addressed with related higher-order mutants of other hormone-involved TCPs. Only 44% of the DEGs in *tcp8* were also affected in *t8t14t15*, with similar distributions seen when comparing grouped TCP-upregulated and TCP-downregulated DEGs (Supplemental Figure S1). This would support the TCP trio having sets of both distinct and common regulatory targets and roles.

Surprisingly, only 6% and 8% of candidates identified by ChIP-seq as having TCP8-bound promoter regions were shown to be differentially expressed in *tcp8* and *t8t14t15*, respectively. Similar observations have previously been made for the related bHLH PIF3 (Zhang et al., 2013), which highlights the complex, likely heterodimeric and additive mechanisms of regulation by TCP8 and other TCPs. The subset of 34 genes bound by TCP8 and differentially expressed in the *tcp8* mutant did not fall into any clear functional or physiological categories but nonetheless represents a valuable resource for direct transcriptional regulatory targets to be pursued individually in future studies (Supplemental Table S4). Specific environmental conditions or hormone treatments may be required to effectively capture these alterations to the transcriptional profile. For the purpose of this study, we continued to focus on more general sectors regulated by TCP8.

A GO term analysis of TCP8- and TCP8/TCP14/TCP15-regulated genes identified significant enrichment of phytohormone signaling genes associated with growth, defense, and light responses in both sets (Figure 1F). The dramatically increased enrichment of JA signaling genes in *t8t14t15* relative to *tcp8* is unsurprising as the suppression of JA and enhancement of SA signaling by TCP14 and TCP15 has been previously described (Yang et al., 2017). We observed a broad pattern of increased enrichment of DEGs associated

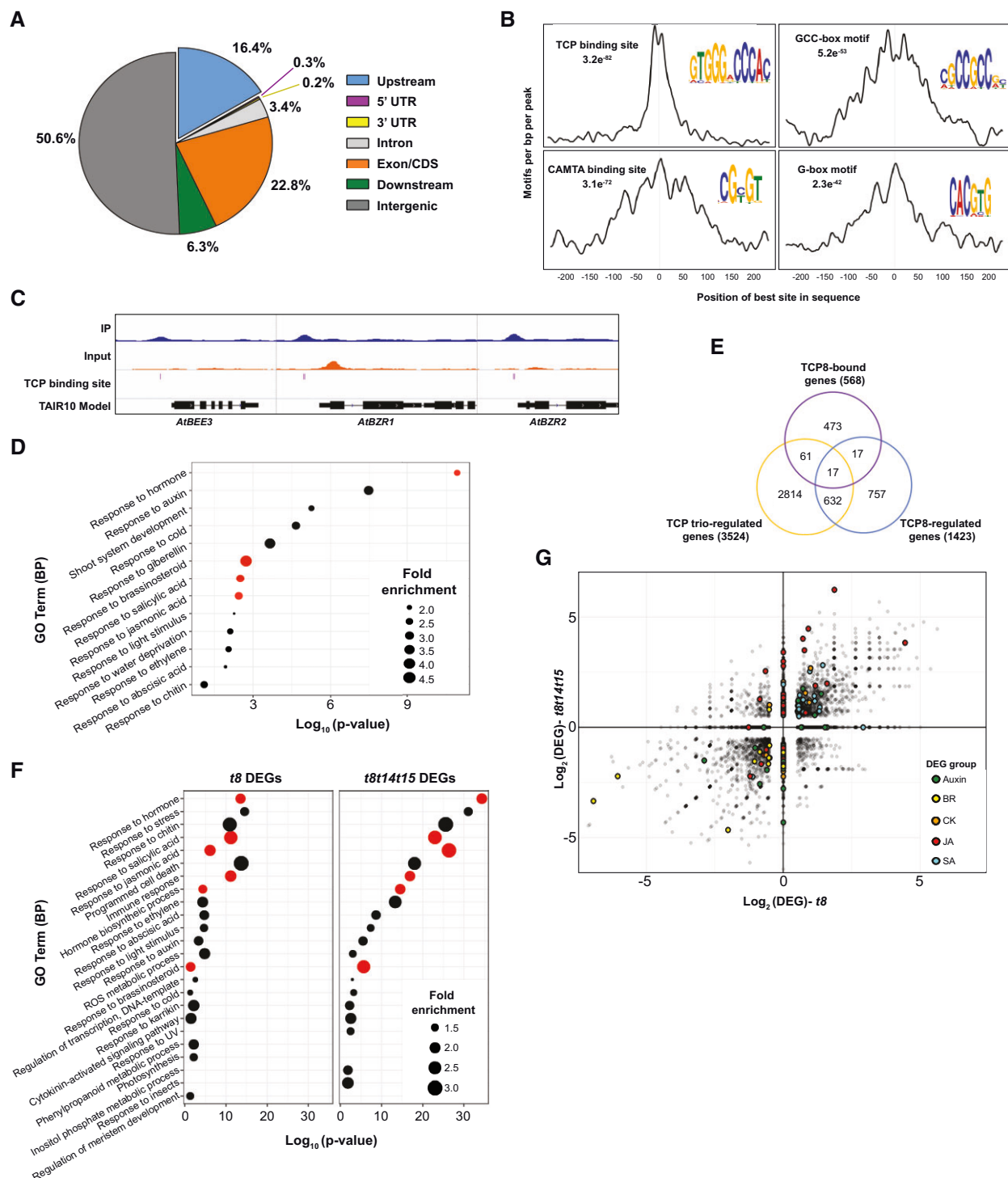


**Figure 1** TCP8 genomic targets are overrepresented in BR and other phytohormone signaling pathways. **A**, Genomic distribution of TCP8 binding peaks, with peaks up to  $\sim 5$  kb classified as upstream. **B**, Enrichment of known TF binding motifs in 250-bp flanking sequences around promoter-localized TCP8 binding peaks was determined by MEME-Suite tools. Highest interesting enriched motifs are represented by sequence logos. **C**, TCP8 binding peaks in representative BR gene promoters *AtBEE3*, *AtBZR1*, and *AtBZR2*. **D**, GO analysis of promoter-localized TCP8-regulated gene candidates.  $\text{Log}_{10}(P\text{-values})$  represented on the x-axis. Significant enrichment determined with  $P < 0.05$  via GoStats. Categories in red are highlighted in the text/are discussed further. **E**, Limited overlap observed between TCP8-bound regulatory targets and *tcp8* DEGs identified by RNA-seq. Greater overlap is observed between *tcp8* and *t8t14t15* DEGs, but the majority of *tcp8* DEGs are exclusive to that genetic background. **F**, GO analysis of TCP8 and *T8T14T15*-regulated genes.  $\text{Log}_{10}(P\text{-values})$  are represented on the x-axis. Categories in red are highlighted in the text/are discussed further. **G**, Scatter plot of  $\text{log}_2$  fold change values in *tcp8*/Col-0 (x-axis) and *t8t14t15*/Col-0 (y-axis) RNA-seq DEGs. Genes associated with phytohormone groups are highlighted (from top to bottom) in green (auxin), yellow (BR), orange (CK), red (JA), or blue (SA).

**Table 1** Phytohormone signaling regulators identified by chIP-sequencing as candidate gene targets of AtTCP8

Tair ID	Gene description	Peak height
<i>Auxin</i>		
AT1G53700	Serine/threonine–protein kinase; WAG1	203
AT5G59430	TELOMERE REPEAT-BINDING PROTEIN 1 (TRP1)	201
AT5G19140	Aluminum-induced protein with YGL and LRDR motifs; AILP1	189
AT3G14370	Serine/threonine–protein kinase; WAG2	176
AT3G04730	Auxin-responsive protein; IAA16	169
AT5G62000	AUXIN RESPONSE FACTOR 2 (ARF2)	159
AT1G15750	TOPLESS (TPL)	150
AT4G37610	BTB/POZ and TAZ domain-containing protein 5; BT5	116
AT3G61830	AUXIN RESPONSE FACTOR 18 (ARF18)	110
AT1G04240	Auxin-responsive protein; IAA3	110
AT4G29080	Auxin-responsive protein; IAA27	104
AT1G35240	AUXIN RESPONSE FACTOR 20 (ARF20)	97
AT2G39550	Geranylgeranyl transferase type-1 subunit beta; GGB	95
AT4G32880	Homeobox-leucine zipper protein; ATHB-8	91
AT4G16780	Homeobox-leucine zipper protein; HAT4	89
AT2G42620	F-box protein; MAX2	85
AT3G48360	BTB/POZ and TAZ domain-containing protein 2; BT2	81
<i>Gibberellin</i>		
AT4G19700	E3 ubiquitin-protein ligase; BOI	178
AT1G76180	Dehydrin; ERD14	123
AT1G69530	Expansin-A1 (EXPA1)	108
AT3G63010	Gibberellin receptor; GLD1B	98
AT3G58070	Zinc finger protein; GIS	90
AT5G11260	LONG HYPOCOTYL 5 (HY5)	72
<i>BR</i>		
AT1G13260	AP2/ERF and B3 domain-containing TF; RAV1	241
AT4G28720	Probable indole-3-pyruvate monooxygenase; YUCCA8 (YUC8)	145
AT2G42870	PHOTOCHROME RAPIDLY REGULATED 1 (PAR1)	134
AT1G75080	BRASSINAZOLE-RESISTANT 1 (BZR1)	125
AT1G19350	BRASSINAZOLE-RESISTANT 2 (BZR2); BES1	124
AT4G39400	BRASSINOSTEROID INSENSITIVE 1 (BRI1)	76
AT5G08130	BES-INTERACTING MYC-LIKE PROTEIN 1 (BIM1)	71
<i>SA</i>		
AT2G04880	WRKY TF 1; WRKY1	120
AT1G80840	WRKY TF 40; WRKY40	112
AT4G05320	POLYUBIQUITIN 10 (UBQ10)	90
AT2G20580	26S proteasome non-ATPase regulatory subunit 2 homolog A; RPN1A	66
AT3G48090	ENHANCED DISEASE SUSCEPTIBILITY 1 (EDS1); EDS1A	58
<i>JA</i>		
AT2G18790	Phytochrome B (PHYB)	101
AT3G15510	NAC TF 56; NAC056	176
AT5G64810	WRKY TF 51; WRKY51	71
AT5G59780	MYB TF; MYB59	56
AT5G10280	MYB TF; MYB92	43
<i>Ethylene</i>		
AT1G06160	Ethylene-responsive TF 94; ERF94	161
AT5G61590	Ethylene-responsive TF 107; ERF107	141
AT1G62300	WRKY TF 6; WRKY6	140
AT1G64060	RESPIRATORY BURST OXIDASE HOMOLOG PROTEIN F (RBOHF)	130
AT3G15210	Ethylene-responsive TF 4; ERF4	125
AT5G38480	14-3-3-like protein GF14 psi; GRF3	118
AT5G25190	Ethylene-responsive TF 3; ERF3	98
AT4G23750	Ethylene-responsive TF; CRF2	75
<i>Abscisic Acid</i>		
AT3G22380	TIME FOR COFFEE (TIC)	205
AT1G20440	Dehydrin; COR47	189
AT1G20450	Dehydrin; ERD10	157
AT3G07360	U-box domain-containing protein 9; PUB9	153
AT1G69270	LRR receptor-like serine/threonine-protein kinase; RPK1	150
AT1G75240	Zinc-finger homeodomain protein 5; ZHD5	132
AT1G56600	GALACTINOL SYNTHASE 2 (GOLS2)	125

with most hormones in the *t8t14t15* background relative to *tcp8*, but this trend is heavily muted for GO pathways like auxin, ABA, and BR, where loss of *TCP8* alone was sufficient to observe similarly weak enrichment of those genes.

A comparison of absolute fold changes relative to Col-0 within a curated list of phytohormone-related DEG candidates in *tcp8* and *t8t14t15* (Figure 1G) also supports the idea of specialization between the TCPs tested. In aggregate, greater degrees of different gene expression were observed for auxin-related genes in *tcp8*, while differences in BR- and SA-related genes were smaller but still significant in that background, CK-related genes were largely uncoordinated, and JA-specific genes were clearly more pronounced in *t8t14t15*. Intersections between the BR and SA signaling pathways are well-established and the known regulation of SA signaling by *TCP8* may uniquely position it to modulate balance of these pathway outputs. We decided to further probe the BR signaling pathway as a test case for candidates identified in the chIP dataset, exploring the possibility of relatively small perturbations of phytohormone-related gene expression levels leading to substantial physiological consequences.

### TCP8 binds and activates BR gene promoters in planta

Putative *TCP8* regulatory targets are associated with perception of BR at the plasma membrane (*BRI1*), transcriptional output (*BZR1*, *BZR2*, *BIM1*, and *BEE3*) and biosynthesis of BR (*BRX*). As class I TCPs have yet to be directly implicated in the regulation of the BR pathway, we explored several of these candidates further to confirm a similar level of regulation by a class I TCP. For a subset of BR signaling candidates, we aimed to verify the chIP-seq results through targeted chIP- quantitative PCR (qPCR) amplification of regions flanking identified TCP-binding sites. Clear enrichment of the target regions of *BZR1*, *BZR2*, and *BRI1* promoters was observed relative to a nontarget region after immunoprecipitation with hemagglutinin (HA)-directed antibody (Figure 2A). Non-BR genes identified in the chIP-seq dataset were also pulled down, here verified by enrichment of the *WRKY40* promoter (Figure 2B).

To determine if the direct interaction between *TCP8* and BR gene promoters is sufficient for their activation, we transiently co-expressed 35S:HA-*TCP8* with promoter:GUS reporter constructs in *Nicotiana benthamiana* (Benth) leaf cells. Through quantification of  $\beta$ -glucuronidase (GUS) activity, we demonstrated that transiently expressed HA-*TCP8* is capable of strongly activating *BZR1* and *BZR2* promoters in planta (Figure 3, A and B). Mutating canonical “GGNCCCA” motifs of two identified TCP-binding sites in the *TCP8*-enriched region of the *BZR2* promoter to “AAAATTT” strongly attenuated activation by HA-*TCP8*. Similar mutations in the *BZR1* promoter showed little effect on its activation, possibly due to the presence of other compensating TCP-binding sites or activities of endogenous TFs that were not interrogated in this study. These data suggest

that *TCP8* directly binds and is sufficient to activate the promoters of several key BR regulatory genes, likely as a positive regulator of BR signaling.

### Enhanced ROS production in the *tcp8* mutant is suppressed by BR treatment

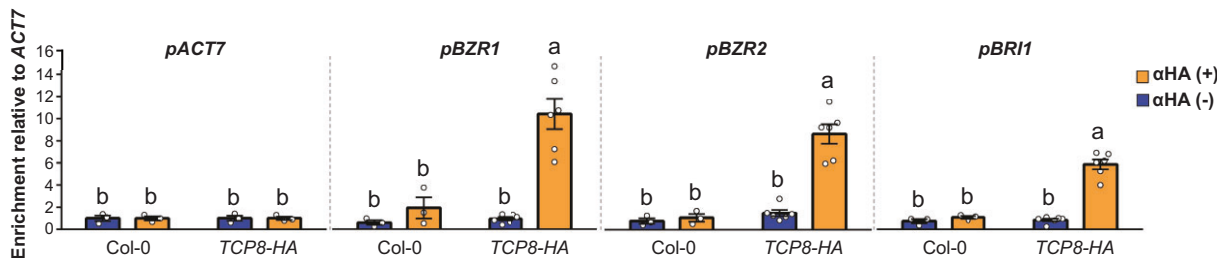
In an earlier study, we observed an increase in *elf18*-induced reactive oxygen species (ROS) production in *t8t14t15*, despite impaired downstream PTI outputs like SA marker gene induction and resistance to pathogen infection (Spears et al., 2019). The tradeoff between growth and defense is demonstrated by a well-established and multileveled antagonism between BR and immune signaling, the mechanisms for which are not yet fully understood but potentially depend on modulation of BZR activities (Belkhadir et al., 2012; Lozano-Duran et al., 2013). We therefore suspected that impaired BR signaling in *tcp8* could be a contributing factor to the enhanced ROS phenotype. In support of this hypothesis, we found that the loss of *TCP8* alone is sufficient for enhanced ROS in a standard leaf disc assay (Figure 4A), and that any differences in response to *elf18* elicitation between WT and *tcp8* were abolished when leaf discs were pretreated with exogenous brassinolide (24-epiBL) (Figure 4, B and C). The observation that *tcp8* exhibits WT levels of downstream (“late”) PTI activation and bacterial growth levels after elicitation (Supplemental Figure S2), but *t8t14t15* levels of enhanced ROS production in upstream (“early”) PTI signaling highlights the separation of immune signaling branches; the lack of additive effect from the loss of *TCP14* and *TCP15* likely reflects a *TCP8*-specific function. Considering our findings that *TCP8* binds and activates BR regulatory genes, these data suggest that this immune signaling phenotype may be caused by a BR signaling deficiency in the *tcp8* background that is restored by the presence of excess BR or compensation by other signaling components.

### TCP8 regulates BR-responsive growth and directly interacts with BZR-family TFs

We reasoned that *tcp8* may exhibit signs of impaired BR signaling, such as altered BR-responsive growth patterns. However, no obvious morphological phenotypes were visible in the *tcp8* mutant, indicating that any insensitivity phenotypes were likely to be mild. Using a standard root growth inhibition assay with 10-day-old *Arabidopsis* seedlings grown on 1/2 Murashige and Skoog (MS), we found that *tcp8* seedlings exhibited relative root length (BL treatment/mock) similar to a BR-insensitive *BZR2* RNAi line and nearly twice the relative length of the fully sensitive Col-0 seedlings when grown on 1/2 MS plates containing 100-nM 24-epiBL (Figure 5A).

We hypothesized that impaired BR signaling in *tcp8* seedlings would result in predisposed sensitivity to inhibition of BR biosynthesis. Accordingly, we measured hypocotyl elongation of etiolated seedlings grown on 1/2 MS plates with 500-nM Brz. We observed a decrease in relative hypocotyl length (Brz/mock) in *tcp8* relative to fully sensitive Col-0

A



B

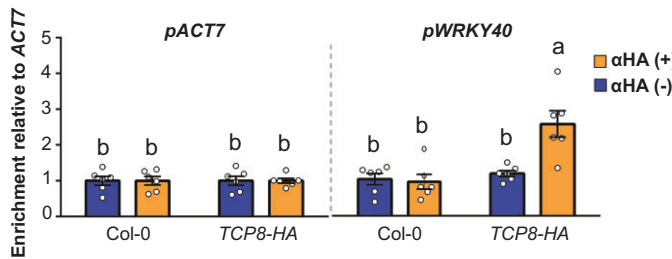


**Figure 2** TCP8-bound BR gene regulatory targets verified by chIP-PCR. A, Chromatin of Col-0 seedlings was immunoprecipitated with either  $\alpha$ HA (HA +) or protein A (HA -) beads and enrichment of BR genes determined relative to the nontarget ACT7 promoter ( $n = 3$  Col-0,  $n = 6$  pT8-T8-HA). B, Verification of WRKY40 promoter occupancy by TCP8 as a representative SA gene candidate. Enrichment of WRKY40 promoter was performed in the same manner as in (A), confirming that regulatory candidates from multiple phytohormone pathways are occupied by TCP8 ( $n = 6$ ). For all chIP-PCR experiments, error bars indicate SE, significance (ANOVA) with Tukey's multiple comparison test, letters denote difference at  $P < 0.05$ .

and the insensitive, constitutively active line *bes1-D*. Again, the *tcp8* phenotype mimics the hypersensitivity of the BZR2 RNAi line (Figure 5B).

To verify that loss of transcriptional activity in *tcp8* contributed to these phenotypes, we collected total mRNA from *Arabidopsis* seedlings grown on 1/2 MS under identical conditions to those in Figure 5A and measured the transcript levels of key TCP8-regulated BR genes. Although low basal BZR1 expression levels likely dampened phenotypic differences, transcript levels were mildly reduced in *tcp8*, while BZR2 transcripts were significantly reduced to nearly half of WT (Figure 5C). Furthermore, the full complementation of the 24-epiBL insensitivity phenotype by the TCP8-HA transgenic line suggests that the activity of TCP8 is sufficient for WT levels of responsiveness to BR (Supplemental Figure S3). Since BZR1/BZR2 transcript levels are severely reduced in the BZR2 RNAi line, it is possible that the *tcp8* phenotype represents a combinatorial effect of mildly reduced transcription at several different BR signaling loci, or perhaps hints at a mechanism by which mild reduction of steady state expression may be phenotypically exacerbated by lack of signal amplification during stress.

The activities of BR-responsive TFs are commonly regulated through interaction with other BR signaling proteins. As an example, in vitro and in vivo interactions with BZR1 and BZR2 have been demonstrated for the PIF family (Oh et al., 2012). TCPs heterodimerize and may form higher-order transcriptional regulatory complexes to regulate their activities (Martin-Trillo and

Cubas, 2010); the co-occurrence of TCP-binding sites with those of other TF families in the immediate area of BR gene promoters such as pBZR2 would point toward this mechanism. Although TCP8 is sufficient to activate BR-responsive gene expression, we hypothesized that TCP8 may form dynamic heteromultimeric regulatory complexes with other G-box binding TFs, such as the BZRs, to finely modulate the expression of these genes.

To explore this idea, we cloned the coding regions of a subset of the BR-related genes identified in our chIP-seq analysis into GST-tagged *Escherichia coli* expression vectors and performed pulldown assays with TCP8. GST-BZR1 and GST-BZR2 co-purified with HIS-T7-TCP8 (Figure 5D), suggesting direct physical interactions between the TFs.

Interactions were verified in planta using a split luciferase assay in *Benthi* leaf epidermal cells. Using a C-terminally tagged TCP8-cLUC construct, interaction was observed with BZR2-nLUC and more weakly interaction with BZR1-nLUC relative to a noninteracting GUS-nLUC control (Figure 5E). The in planta results largely mirror the interactions observed in the *E. coli* system. These data point toward a model by which TCP8 directly regulates transcriptional control of BR signaling pathways through direct and genetic interactions with master regulators BZR1 and BZR2.

#### TCP8 subnuclear localization and activities are BR-responsive

TCP8 and other class I TCP TFs have been observed to form nuclear condensates basally or as an induced response to

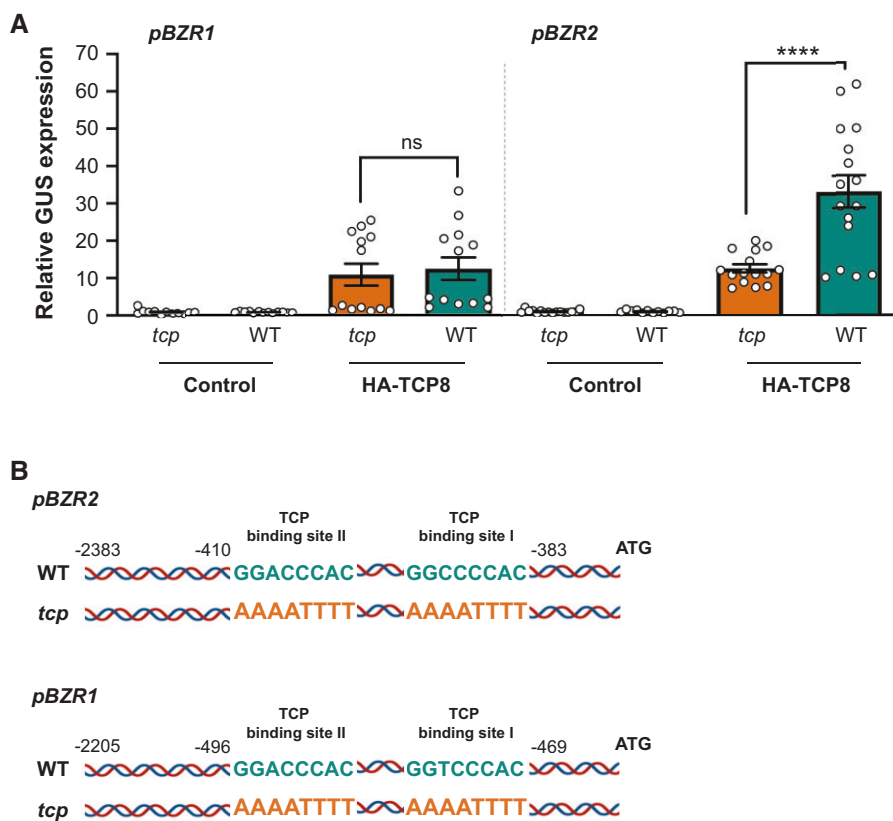


**Figure 3** TCP8 transactivates *pBZR2* promoter:GUS construct in a TCP-binding site dependent manner in *Benthii*. A, GUS expression relative to control was determined by 4-MUG assay after co-expression of reporter construct and EV (control) or HA-TCP8 construct in *Benthii* cells and data combined from three independent experiments. Error bars indicate SE, \*\*\*P < 0.0001 (n = 13–16, Student's t test). B, Model of the WT and TCP-binding site mutant (*tcp*) promoter versions tested in the *pBZR1* and *pBZR2* GUS reporter constructs.

various protein–protein interactions and stresses (Valsecchi et al., 2013; Kim et al., 2014; Mazur et al., 2017; Yang et al., 2017; Perez et al., 2019). The nature of these subnuclear localizations has yet to be explored, but could be sites of suppression, enhanced activation, or both at multiple genetic loci. BR-responsive TFs like the bHLH protein CESTA form similar nuclear condensates in a BR-dependent manner (Poppenberger et al., 2011). To determine the effect of brassinolide perception on the cellular localization of TCP8, 35S:GFP-TCP8 was transiently expressed in *Benthii* leaf epidermal cells and the infiltrated tissue was treated with 2-μM Brz in order to reduce levels of endogenous BR signaling and gene expression. In Brz-treated cells, the proportion of nuclei exhibiting punctate localization of GFP-TCP8 was reduced relative to the mock treatment. However, elicitation of the Brz-treated cells with 1-μM 24-epiBL partially restored basal localization patterns, while a control treatment largely had no effect (Figure 6A). These trends corresponded with the quantified mean number of condensates per nucleus for each treatment. The data indicate BR perception may direct a portion of mature TCP8 protein into nuclear condensates and that endogenous levels of BR signaling may account for reports of similar TCP8 localization patterns without specific elicitation. The finding that Brz treatment also reduces interaction between TCP8 and BZR2 (Supplemental Figure S4)

would support these condensates as sites of their interaction in the presence of BR.

In the case of CESTA, its BR-dependent movement into nuclear bodies is thought to suppress activation of BR gene expression (Khan et al., 2014). Along those lines, we explored the effects of Brz treatment on the transactivation by TCP8 in *Benthii*. Interestingly, we observed increased activation of the *pBZR2* reporter construct by HA-TCP8 when leaves were treated with 2-μM Brz (Figure 6B). Total TCP8 abundance was unchanged by the treatment both in *Benthii* (Figure 6C) and in the native promoter-driven *Arabidopsis* TCP8-HA line (Supplemental Figure S5), confirming that changes in relative activity were not a consequence of reduced protein levels. Excitingly, we also observed the same nuclear condensates to be sites of colocalization between fluorescently tagged GFP-TCP8 and RFP-BZR2 (Figure 6D; Supplemental Figure S6). Our data suggest a potential function of these bodies in the repression of TCP8 activities, likely regulated through interactions with BZR2 and other TFs in the context of BR signaling.

## Discussion

The involvement of TCP8 and other class I TCPs in SA-dependent immune responses has been established in multiple recent studies, in part contributing to the family's rise to

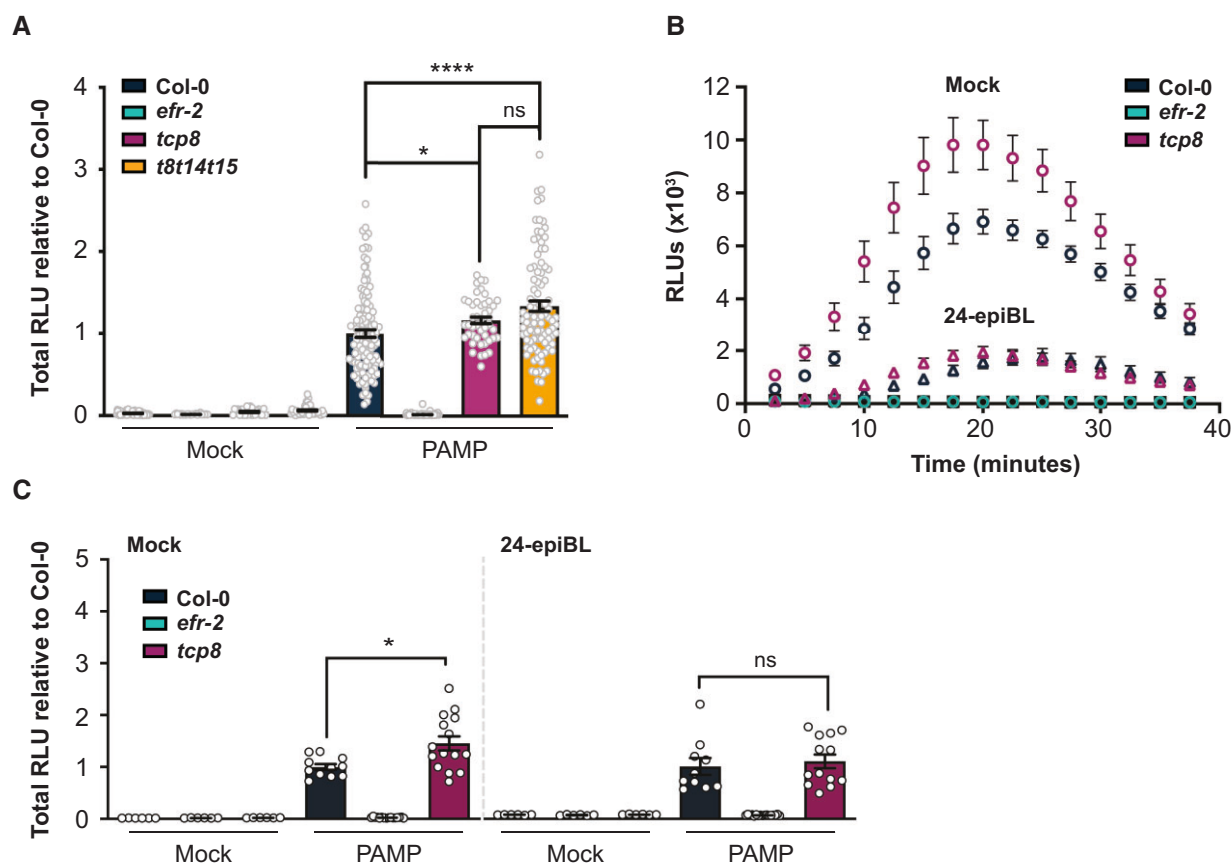


**Figure 4** Enhanced elf18-induced ROS production in *tcp8* is suppressed by BR treatment. **A**, ROS production was elevated in *tcp8* relative to Col-0, but unchanged relative to *t8t14t15* after treatment with 1  $\mu$ M elf18 (PAMP). Total RLU were determined relative to Col-0 and data combined from five independent experiments, error bars indicate  $\text{SE}$ , \* $P < 0.05$ , \*\*\*\* $P < 0.0001$  ( $n > 46$ , Student's  $t$  test). **B**, In time course experiments, observed differences in ROS production between Col-0 and *tcp8* were attenuated by 24-h pretreatment with brassinolide (1  $\mu$ M 24-epiBL) or mock (circles mock, triangles BL treatment). Error bars indicate  $\text{SE}$  ( $n = 12$ –16). Similar results were observed for three independent experiments. **C**, Total RLU measurements from (B) time course normalized to Col-0. Error bars indicate  $\text{SE}$ , \* $P < 0.05$  ( $n = 12$ –16, Student's  $t$  test).

prominence as a potential pathogen-targeted signaling hub. In one example, TCP14 is destabilized by the *Pseudomonas syringae* (*Pst*) effector HopBB1 to antagonistically suppress SA and promote the virulence of the hemibiotrophic pathogen (Yang et al., 2017). More recently, TCP8 was demonstrated to be targeted by multiple effectors of another hemibiotroph, *X. campestris* *pv. campestris* (*Xcc*), but mechanisms of virulence have yet to be explored (González-Fuente et al., 2020). For any pathogen, virulence requirements extend beyond suppression of host immunity—this begs the question of what else these TCPs may be doing that make them such attractive targets. To fully understand the role of TCPs in these interactions, higher resolution of their transcriptional targets is required. We performed ChIP-seq in this study with the goal of complementing our previous data supporting TCP8 as an effector target for its direct role in PTI. Several defense genes were identified as TCP8 regulatory targets in our ChIP-seq dataset, including WRKY-family TFs (WRKY1, WRKY40, and WRKY51), ENHANCED DISEASE SUSCEPTIBILITY 1 (EDS1), and the NADPH oxidase *RbohF* (Table 1). Notably absent among the regulatory candidates is the receptor gene *EFR*, which is directly activated by TCP8

in response to elicitation by the PAMP elf18 (Spears et al., 2019). It is possible that untargeted ChIP-seq may require elicitation to observe enrichment of that particular locus, or that we did not fully capture the scope of TCP8 binding targets with our use of a lower expression, native promoter-driven TCP8 transgenic line. This is perhaps reflected by the relatively low representation of bound defense gene promoters. A more complex model of gene regulation fits the limited overlap between our ChIP-seq and RNA-seq data sets (a common observation). These binding sites may represent promoters that are bound but not constitutively activated or repressed, in wait of the appropriate stimulus, posttranslational modification (PTM) of TCP8, or activation of a necessary co-regulating TF partner as described for some WRKY TFs (Mao et al., 2011).

Interestingly, the list of regulatory candidates was dominated by hormone signaling pathway components, particularly those associated with auxin, gibberellin, and BR signaling. This may point toward a role for TCP8 not as a primary regulator of any one particular phytohormone pathway, but rather as a regulator of baseline hormonal balancing across pathways; interactions with additional TF groups

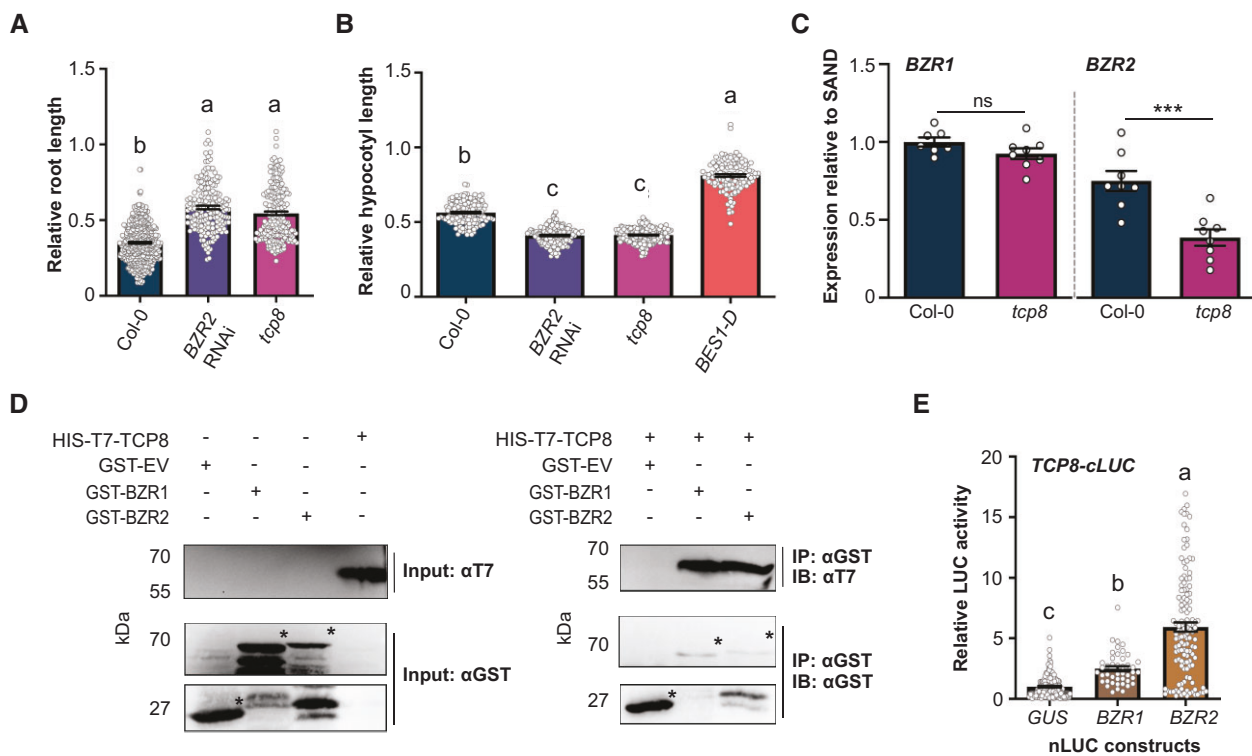


**Figure 5** TCP8 controls BR-responsive growth patterns and interacts with BZR1 and BZR2. **A**, Seedlings were grown on 1/2 MS plates containing DMSO (mock) or 100-nM 24-epiBL in long-day growth conditions for 10 days. Proportional root length (BL treatment relative to mock) was determined for each genotype tested. Similar enhanced growth relative to Col-0 was observed in *tcp8* as in the BL-insensitive *BES1/BZR2* RNAi line ( $n > 184$ ). **B**, Seedlings were grown on 1/2 MS plates containing DMSO or 500-nM Brz in darkness for 8 days. Proportional hypocotyl length (Brz treatment relative to mock) was determined for each genotype tested. Similar Brz hypersensitivity relative to Col-0 was observed in *tcp8* as in the *BES1/BZR2* RNAi line, while the opposite effect was observed in dominant *bes1-D* mutant control line ( $n > 134$ ). For sensitivity experiments, bars indicate 1 se, significance (ANOVA),  $P < 0.01$  with Tukey's multiple comparison test. **C**, Transcript levels of BZR2 are significantly reduced in *tcp8* relative to Col-0. Total RNA was collected from 10-day-old seedlings grown under identical conditions as in (A). Expression levels normalized to the housekeeping gene SAND ( $n = 8$ ). Error bars indicate se, significance (ANOVA) with Tukey's multiple comparison test; letters denote difference at  $P < 0.001$ . **D**, In vitro interaction of HIS-T7-TCP8 with GST-BZR1 and GST-BZR2. The experiment was repeated three times with similar results. **E**, TCP8 interacts with BZR1 and BZR2 in planta. Interactions were evaluated by split-luciferase assay in *Benthi* leaf epidermal cells. Total RLUs were normalized to noninteracting control (*nLUC-GUS*) levels as relative luciferase activity and data combined from three independent experiments. Error bars indicate 1 se, significance (ANOVA) with Tukey's multiple comparison test; letters denote difference at  $P < 0.01$  ( $n > 130$ ).

such as PIFs or BZRs may allow fine-tuning or specialization of TCP8 activity in response to environmental signals. This would support the proposed role of TCP8 and other class I TCPs as central signaling hubs, as well as ideal pathogen targets for manipulation of host hormone levels as a virulence mechanism.

In this manuscript, we focused primarily on the BR branch of regulatory candidates highlighted in the chIP-seq dataset, but the data sets generated will allow for additional studies to explore the involvement of TCP8 in other represented phytohormone pathways. Specifically, we describe a previously uncharacterized role of TCP8 as an activator of multiple key BR master regulators, with activities and localization patterns controlled by cellular BR levels. These data highlight a TCP8-specific role that broadly contrasts with previously described functions. However, our data are in line with previous observations about its regulatory target BZR2 which is capable of promoting both BR-responsive gene expression and PTI-related gene expression, depending on the kinases it

associates with and phosphorylation status at different residues (Kim et al., 2009; Kang et al., 2015). Mechanisms controlling its activation of multiple possible hormone-related signaling pathways are a key point of interest. One possibility is that TCP8 promoter occupancy switches between different hormone-responsive regulatory targets in response to local signals. Another could involve a core set of gene promoters that are involved in promoting multiple hormone signaling pathways themselves; a third mechanism previously described may include further regulation by combinatorial interactions between TCP8 and other TFs. These possibilities are by no means mutually exclusive.

It is possible that other TCP family or bHLH proteins may contribute to this phenotype by acting as a determining factor of which regulatory targets and pathways are activated by TCP8 under certain conditions. As with the regulation of skotomorphogenesis in the related PIF family (Zhang et al., 2013), TCP8 likely acts in concert with other TFs to cooperatively regulate a core set of BR genes at the level of

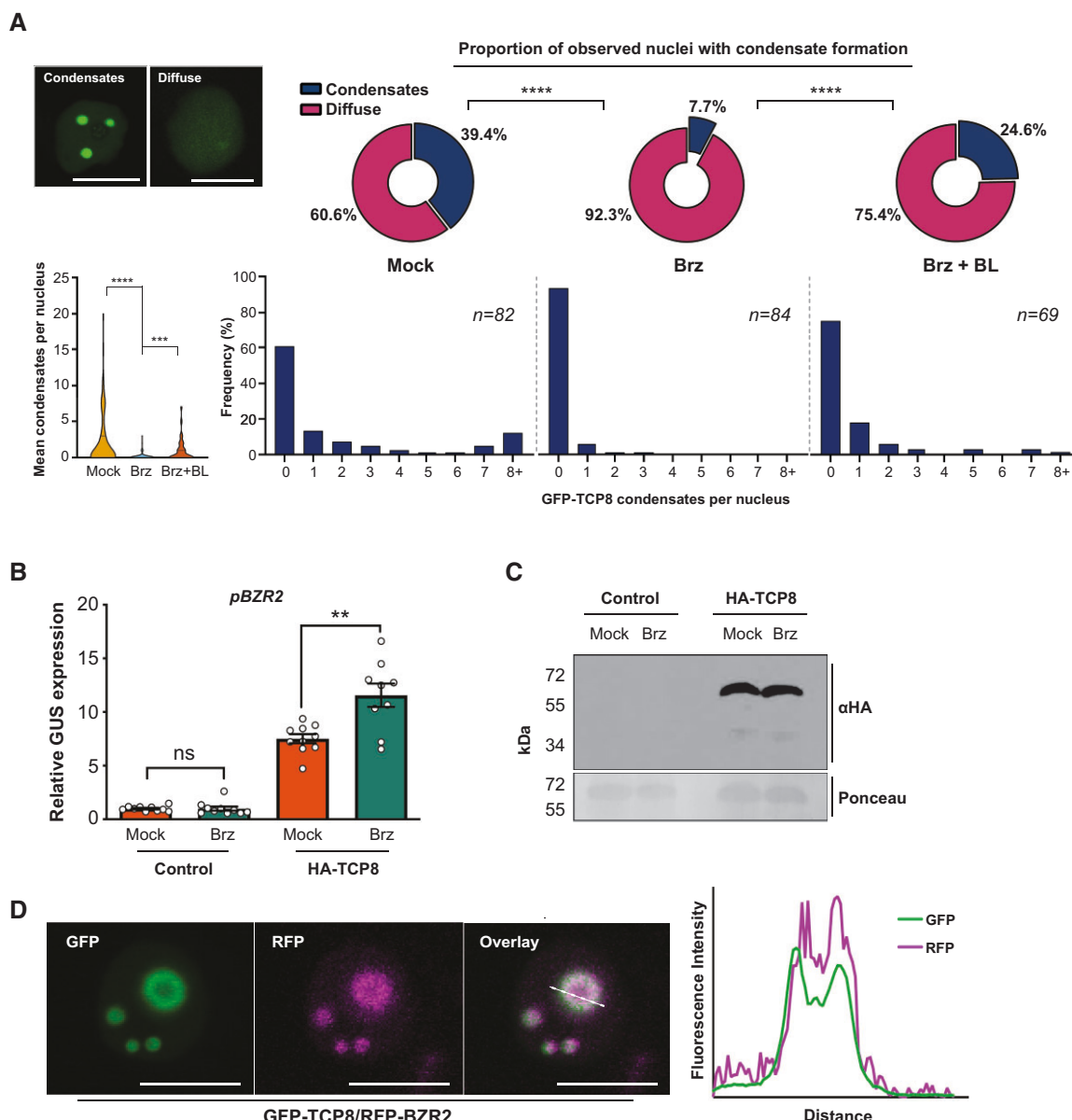


**Figure 6** BR influences localization and activity of TCP in Benthii. A, 35S:GFP-TCP8 was expressed in Benthii leaf epidermal cells and leaves treated with either 2- $\mu$ M Brz or DMSO mock solution, and then re-infiltrated with 1- $\mu$ M brassinolide (BL) solution. For nuclei with visible GFP signal, a significantly lower proportion of nuclei exhibited nuclear condensates after Brz treatment as compared to mock. Reapplication of 24-epiBL partially restored condensate occurrence to normal levels. Samples collected across three experimental replicates.  $P < 0.0005$  ( $n > 69$ , Chi-Square Test for Association). Identical relationships were observed in measurements of mean condensate number per nuclei for each treatment. \*\*\* $P < 0.001$ , \*\*\*\* $P < 0.0001$  (Student's  $t$  test). Scale bars are 10  $\mu$ m. B, Brz treatment enhances transactivation of the *pBZR2* promoter:GUS construct in Benthii. GUS expression relative to control was measured after 24-h pretreatment with 2- $\mu$ M Brz or mock solution. Significantly higher GUS expression was observed in the Brz-treated leaf samples as compared to the mock treatment. Error bars indicate 1 SE, \*\* $P < 0.01$  ( $n = 10$ , Student's  $t$  test). C, Total protein was isolated under the same conditions and HA-TCP8 protein levels analyzed by western blot with  $\alpha$ HA antibody. Treatment with 2- $\mu$ M Brz had no visible effects of TCP8 protein level relative to DMSO mock. Similar results were observed in two independent experiments. D, 35S:GFP-TCP8 and 35S:RFP-BZR2 were co-expressed in Benthii leaf epidermal cells and observed for colocalization. Fluorescence intensity determination across a manually selected plane reveals strong colocalization within the observed nuclear condensates. Scale bars are 10  $\mu$ m. Similar results to these representative images were observed in three independent experiments.

hormone biosynthesis, signal transduction, and response. This is further supported by the finding that ~25% of our identified TCP8-bound gene promoters (Supplemental Table S5) are also bound by BZR1 or BZR2 (Sun et al., 2010; Yu et al., 2011) and the observed in vitro and in planta

interactions with BZR1 and BZR2 (Figure 5). Consistent with bHLH activities (Pireyre and Burow, 2015), combinatorial interactions with TF families regulating SA, auxin, or ABA signaling may contribute to the regulation of diverse biological processes by TCP8 that is reflected in our sequencing

data. From the overabundance of auxin-responsive gene candidates identified in our chIP analysis (Figure 1), a role for TCP8 in auxin signaling would be particularly interesting in the context of this study due to known cooperation between auxin and BR and antagonism between auxin and SA that is thought to be exploited by pathogens as a virulence mechanism (McClerkin et al., 2018; Kong et al., 2020).

In the presence of BR, TCP8 may homodimerize or interact with TFs like BZR1 or BZR2 in heteromultimeric complexes. Our data support a model by which increased concentrations of BR induce the movement of TCP8 into regulatory nuclear condensates to modulate BR-responsive gene expression. As BR levels are reduced, TCP8 may associate more weakly with repressive complexes, contributing to a generally diffuse localization pattern. In this state TCP8 can freely activate baseline subsets of BR genes, such as BZR2, to replenish hormone levels and activate other signaling responses induced under low-BR conditions (Figure 7). Similar instances of phase separation have already been characterized for transcriptional regulators of multiple phytohormone pathways (Powers et al., 2019; Zavaliev et al., 2020; Zhu et al., 2021). Although further study is required to clarify mechanisms and functions of TCP8 condensate formation, including the role of TCP/BZR dimerization in the activation of BR gene expression, there is an intriguing possibility of similar induction by other TCP8-involved hormone signaling pathways. Additionally, as with the BR-dependent

subnuclear localization of the bHLH CESTA (Khan et al., 2014), the formation of TCP8 condensates is likely regulated posttranslationally. These findings highlight the potential importance of previously described TCP8 phosphosites (Xu et al., 2017) and sumoylation (Mazur et al., 2017) to its function in BR signaling. By this regulatory mechanism, TCP8 may act dynamically as one component of an elaborate “switch” between different transcriptional priorities induced by a plant’s perception of defense or growth signals, or the yet uncharacterized manipulations of interacting pathogen effectors aiming to modulate phytohormone signaling outputs.

## Materials and methods

### Plant material and cultivation

Arabidopsis (*A. thaliana*) plants used in chIP-qPCR, chIP-seq, and RNA-seq experiments were grown in liquid 1/2 MS media on a light rack under 24-h light at room temperature. All other Arabidopsis plants were grown on soil or 1/2 MS 0.8% w/v phytoagar plates in an E-7/2 reach-in growth chamber (Controlled Environments Ltd.) under an 8-h light and 16-h dark cycle at 24°C, 70%–80% relative humidity, and a light intensity of 140–180- $\mu$ mol photons per square meter per second. Benthic (*N. benthamiana*) plants used in transactivation, interaction, and localization assays were grown under an 8-h light and 16-h dark cycle at 22°C and 55% relative humidity.

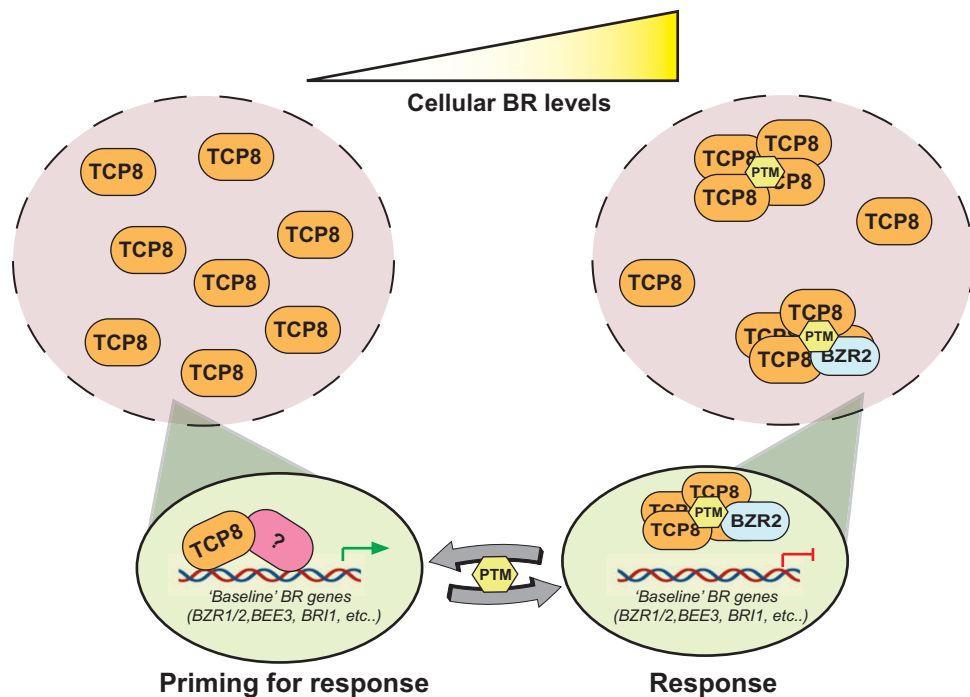


**Figure 7** A working model for regulation of BR signaling by TCP8 in Arabidopsis. At low levels of cellular BR, TCP8 associates with the promoters of “baseline” BR genes to prime the cell for production of and response to BRs. At high levels of cellular BR, TCP8 involvement in the activation of BR signaling is no longer necessary, and excess TCP8 protein enters nuclear condensates, producing the “punctate” nuclear phenotype observed in this study. Both the formation of these condensates and the described interactions with BR regulators BZR1 and BZR2 under basal conditions are likely dynamically regulated through post-PTMs of TCP8. Although the function of these nuclear condensates remains to be explored, our data suggest they may be repressive in nature.

The transgenic *pTCP8:TCP8-HA* (Spears et al., 2019), *tcp8-1* and *tcp* triple mutant (Kim et al., 2014), *efr-2* mutant (Zipfel et al., 2006), *BZR2* RNAi (Yin et al., 2005), and *bes1-D* (Yin et al., 2002) lines have all been previously characterized.

### Molecular cloning

Full-length cDNAs of *BZR1* and *BZR2* without stop codons were amplified from cDNA template synthesized from Col-0 gDNA and cloned into the Gateway-compatible donor vector pDONR201 (Invitrogen, Waltham, MA, USA). *GUS* and *BR* gene donor clones were moved by LR reaction into split luciferase vector pCAMBIA-NLUC, while a *TCP8* donor clone was moved into pCAMBIA-CLuc (Chen et al., 2008).

GFP-TCP8 and RFP-BZR2 constructs were made by Gateway LR reaction (Invitrogen) from pDONR201 clones into pMDC83 (Curtis and Grossniklaus, 2003) and pSITE-4CA (Chakrabarty et al., 2007), respectively.

*BR* gene donor clones were used as template for PCR-based addition of BamHI and SmaI restriction sites to the CDS. Products were digested and ligated into corresponding restriction sites in the GST-tag vector pGEX-4T3 (GE Healthcare, Chicago, IL, USA).

For transactivation experiments, 2-kb upstream regions of *BZR1* and *BZR2* were cloned into pDONR201. Mutant *tcp* variants of the promoters were generated by site-directed mutagenesis. Donor clones were moved by Gateway LR reaction into pYXT1 (Xiao et al., 2005) to produce complete promoter-reporter constructs.

### Assays in Benthii expression system

For transactivation assays, *Agrobacterium* (*Agrobacterium tumefaciens*) strain GV3101 was electroporated with various promoter:GUS constructs, and strain C58C1 electroporated with a 35S:HA-TCP8 construct (Kim et al., 2014). Overnight cultures were generated for each transformant at 30°C, then pelleted and resuspended in 10-mM MgCl<sub>2</sub> buffered with 1-mM MES (pH 5.6) and 100-nM acetosyringone (3',5'-dimethoxy-4'-hydroxyacetophenone). Suspensions were incubated for 4–5 h. Bacterial inocula were mixed to an optical density at 600 nm of 0.2 for each strain and syringe infiltrated into mature Benthii leaves. Tissue was collected 72 h after inoculation with a 1-cm diameter hole punch, 4 leaf discs per sample. Protein was isolated in extraction buffer and GUS quantified according to a standard 4-MUG assay. Protein concentration was determined by Bradford assay and GUS levels calculated before normalization to the empty vector control. For Brz treatments, infiltrated leaves were then gently re-infiltrated with either a DMSO mock or 2-μM Brz solution, before incubating for an additional 24 h.

Immunoblot analysis of epitope-tagged TCP8 in Benthii and Arabidopsis was performed by extracting one gram of total protein in 1 mL of 2× sodium dodecyl sulfate (SDS) buffer (100-mM Tris-HCl, pH 6.8, 4% w/v SDS, 20% v/v glycerol, 250 mM dithiothreitol). Samples were cleared by centrifugation at 16,000 × g and loaded onto an 8% v/v bis-acrylamide SDS-polyacrylamide gel electrophoresis gel.

Protein was detected with 1:2,000 horseradish peroxidase-conjugated anti-HA antibody (Roche, Basel, Switzerland).

### BR localization assays

For BR localization assays, constructs were transformed into *Agrobacterium* C58C1 and inocula prepared at an OD<sub>600</sub> of 0.05. Benthii leaves were syringe infiltrated and incubated for 48 h under standard conditions. For elicitor treatments, infiltrated leaves were then gently re-infiltrated with either a mock (DMSO) or 2-μM Brz solution, before incubating for an additional 24 h. Then 2 h prior to observation under a Leica TCS SP8 microscope, leaves were infiltrated once more with either a DMSO mock or 1-μM 24-epiBL solution.

Nuclei with visible GFP signal were randomly sampled (three experimental replicates, ~10–15 images, >20 nuclei per rep) and GFP-TCP8 localization status determined for each. Nuclei were scored for presence (1) or absence (0) of visible nuclear condensates from collected z-stacks and effects of treatment on localization was determined by a Chi-square Test of Association. Mean numbers of condensates per nuclei were quantified from the same images and analyzed by Student's *t* test.

### Colocalization assays

Leaf discs were imaged using a Zeiss LSM710 inverted confocal microscope with a 40×/1.2 water objective. For colocalization analysis, GFP was excited using an argon laser with peak excitation at 488 nm at 2% intensity. Emission from GFP was collected between 500 and 550 nm with gain of 400. RFP was excited with a DPSS laser at peak excitation of 561 nm and 11% intensity. RFP emission was collected between 560 and 620 nm at gain of 800. Single Z-plane images from both laser channels were captured and then colocalization was analyzed using Fiji (ImageJ). A region of interest was selected using the Straight Line tool and fluorescence intensity was measured using the Plot Profile feature.

### chIP and chIP-seq analysis

chIP was performed with 10-day-old seedlings grown in liquid 1/2 MS as previously described (Spears et al., 2019). For chIP-PCR, 5 μL of the resulting purified DNA was analyzed by qPCR as described above. For chIP-seq, chIP DNA and input DNA from five biological replicates were used to construct libraries with an NEBNEXT Ultra II Kit Library prep kit according to the manufacturer's protocol. High-throughput sequencing of prepared libraries was performed on an Illumina NextSeq 500.

Processed FASTQ sequences were mapped to the *Arabidopsis* TAIR10 genome using Bowtie2 (<http://bowtie-bio.sourceforge.net/bowtie2/index.shtml>). Nonuniquely mapped reads were removed, and enriched TCP8-binding peaks were called from pooled chIP/input files using MACS2 (<http://github.com/downloads/taoliu/MACS/MACS-1.4.2-1.tar.gz>) with estimated fragment size 189, shift size 0, and cutoff (FDR < 0.05).

Genome distribution of called peaks was determined by the PAVIS tool (<https://manticore.niehs.nih.gov/pavis2/>) with

upstream and downstream limits set to 3,000 bp and 1,000 bp, respectively.

Motif analysis of promoter-bound TCP8 binding peaks was performed using the MEME-Suite tools (<https://meme-suite.org/meme/tools/meme>). From upstream peak coordinates, 250-bp flanking sequences (500-bp total) were determined and analyzed using default settings.

GO term analysis was performed using the DAVID platform (<https://david.ncifcrf.gov/>).

### RNA-seq and analysis

RNA was isolated from 10-day-old seedlings grown under identical conditions as the ChIP-seq experiments. Libraries were prepared using an Illumina TruSeq stranded library preparation kit according to manufacturer's protocol. High-throughput sequencing of prepared libraries were performed on an Illumina NextSeq 500 and analysis was performed as previously described (McInturf et al., 2022).

Briefly, after sequencing adapters were removed, bases at the 5'- and 3'-end of each read were removed such that the confidence scores of each base in the remaining read were each >99%. These trimmed reads were then mapped to the TAIR10 genome release using the ShortRead Package in R Bioconductor. Differential expression was assessed using the edgeR package, using tagwise dispersion estimates and Bonferroni and Hochberg multiple testing correction.

Ontology enrichment was performed using the GOStats package (Falcon and Gentleman, 2007). The background frequency for each ontology (gene universe) was defined to be the union of all genes with (uncorrected)  $P \leq 0.05$ , and all pairwise comparisons were made between genotypes.

### RT-qPCR

RNA was isolated from whole 10-day-old seedlings under etiolating conditions and reverse transcription performed according to manufacturer specifications. Reverse transcription quantitative PCR (RT-qPCR) was performed with 5  $\mu$ L of 20  $\times$  -diluted cDNA and a primer concentration of 1  $\mu$ M in a 20- $\mu$ L reaction with Brilliant III Ultra-Fast SYBR GREEN Master Mix (Agilent Santa Clara, CA, USA) with a BioRad CFX Connect thermocycler (Bio-Rad, Hercules, CA, USA). Transcript levels were normalized to the housekeeping gene SAND.

### Arabidopsis BL/Brz sensitivity assays

BL sensitivity was evaluated by a standard root-length assay. Stratified seed was plated on square 1/2 MS plates with either mock DMSO or 100-nM 24-epiBL (Sigma E1641). Plates were placed vertically at 4°C for 2 days with foil covering before removal of foil and transfer to a short-day growth chamber. Seedlings were grown for ~10 days before root length was measured using ImageJ.

Brz sensitivity was evaluated by a similar protocol to measure etiolated hypocotyl elongation. Briefly, stratified seed was plated on square 1/2 MS plates with either mock DMSO or 500-nM Brz (Sigma SML1406). Plates were covered in foil and placed vertically at 4°C for 2 days before

removing the foil and transferring plates to a short-day growth chamber for 3 h. Plates were then covered again in foil and seedlings were grown for 8 days before hypocotyl length was measured using ImageJ.

### Arabidopsis immunity assays

ROS production was measured by a standard H<sub>2</sub>O<sub>2</sub>-dependent luminescence assay (Heese et al., 2007) with modifications. Briefly, 1-cm diameter *Arabidopsis* leaf discs were halved and then floated in 100- $\mu$ L water with either DMSO or mock or 1- $\mu$ M 24-epiBL added in a 96-well plate under full light overnight. Incubation solution was removed and replaced with 100-nM elf18 or DMSO mock elicitation solution. Luminescence was quantified in 2-min increments over a 30-min period immediately after elicitation.

Bacterial growth assays were performed as previously described (Spears et al., 2019).

### Protein interaction assays

In vitro co-pulldown assays with GST-EV/BZR1/BZR2 and His-T7-TCP8 were performed as previously described (Halane et al., 2018). Briefly, GST-tagged proteins were pulled down, incubated with HIS-T7-TCP8 lysate, and eluted from binding columns before probing with  $\alpha$ T7 and  $\alpha$ GST antibodies.

In planta split luciferase assays were performed according to a standard protocol (Cazzonelli and Velten, 2006) with modifications. Briefly, GUS/BZR1/BZR2-nLUC and TCP8-cLUC constructs were transformed into *Agrobacterium* C58C1 and co-inoculated at OD<sub>600</sub> 0.2 into *Benthi* leaves by syringe infiltration. After 72 h, leaf discs were taken by a sharp 0.5-cm diameter (#2) bore and floated abaxial side down on 100- $\mu$ L infiltration solution (50-mM MES pH 5.6, 10-mM MgCl<sub>2</sub>, 0.5% DMSO) in a white 96-well plate with lid. Plates were wrapped in foil and incubated in a growth chamber for 20 min. Infiltration solution was removed by multipipettor and replaced with 100- $\mu$ L reaction solution (1  $\times$  infiltration solution, 1-mM luciferin (Goldbio, St Louis, MO, USA; #LUCK-100)). Luminescence was quantified in 10-min increments over a 2-h period in a BioTek Synergy HTX plate reader.

### Accession numbers

The TAIR accession numbers for referenced genes are as follows:

At1g09530 (PIF3), At1g19350 (BZR2), At1g25330 (CESTA), At1g31880 (BRX), At1g58100 (TCP8), At1g69690 (TCP15), At1g73830 (BEE3), At1g74710 (ICS1), At1g75040 (PR5), At1g75080 (BZR1), At1g80840 (WRKY40), At2g28390 (SAND), At3g47620 (TCP14), At4g16890 (SNC1), At4g39400 (BRI1), At5g20480 (EFR), and At5g46330 (FLS2). The sequencing data used in this study are openly available in the NCBI SRA at <https://www.ncbi.nlm.nih.gov/sra>, accession number PRJNA754790.

## Supplemental data

The following materials are available in the online version of this article.

**Supplemental Figure S1.** Venn diagrams of class I TCP regulatory target groups.

**Supplemental Figure S2.** Bacterial growth levels are unaffected in *tcp8* relative to Col-0.

**Supplemental Figure S3.** Affected BR-responsive growth patterns are restored in the *TCP8-HA* complemented line.

**Supplemental Figure S4.** Interactions between TCP8 and BZR2 are disrupted by Brz treatment.

**Supplemental Figure S5.** TCP8 protein levels are unaffected by cellular BR levels in *Arabidopsis*.

**Supplemental Figure S6.** Evaluation of signal specificity for colocalization assay.

**Supplemental Table S1.** TCP8 binding peaks identified by ChIP-sequencing.

**Supplemental Table S2.** TCP8 binding peaks categorized by genomic location.

**Supplemental Table S3.** DEGs identified by RNA-sequencing in *tcp8* and *t8t14t15*.

**Supplemental Table S4.** TCP8-bound DEGs identified by RNA-sequencing in *tcp8* and *t8t14t15*.

**Supplemental Table S5.** Comparison between known TCP8 and BZR gene promoter targets.

**Supplemental Table S6.** Primers used in this study.

## Acknowledgments

We are grateful to C. Garner for technical advice and microscopy assistance and to P. Martin and M. Creach for plant maintenance and general assistance. Thanks to the University of Missouri Molecular Cytology Core for technical assistance and setup involved in acquiring confocal images presented in this study. Thanks also to the Indiana Biosciences Research Institute for housing the Marian University satellite laboratory and use of confocal microscope. Many thanks to M.Y. Zhou and the University of Missouri Genomics Technology Core for technical support and services involved in Illumina library preparation and sequencing.

## Funding

The work presented here was supported by a BSI Award from Butler University (to M.C.), a Holcomb Awards Committee (HAC) Faculty Research Grant from Butler University (to B.J.S.), an MU Plant Sciences Daniel F. Millikan Fellowship (to B.J.S.), and by US National Science Foundation Integrative Organismal Systems program grants (IOS-1121114 and IOS-1456181 to W.G.).

*Conflict of interest statement.* None declared.

## References

**Ahmed H, Howton TC, Sun Y, Weinberger N, Belkhadir Y, Mukhtar MS** (2018) Network biology discovers pathogen contact points in host protein-protein interactomes. *Nat Commun* **9**: 2312

**Albrecht C, Boutrot F, Segonzac C, Schwessinger B, Gimenez-Ibanez S, Chinchilla D, Rathjen JP, de Vries SC, Zipfel C** (2012) Brassinosteroids inhibit pathogen-associated molecular pattern-triggered immune signaling independent of the receptor kinase BAK1. *Proc Natl Acad Sci USA* **109**: 303–308

**Belkhadir Y, Jaillais Y, Epple P, Balsemao-Pires E, Dangl JL, Chory J** (2012) Brassinosteroids modulate the efficiency of plant immune responses to microbe-associated molecular patterns. *Proc Natl Acad Sci USA* **109**: 297–302

**Cazzonelli CI, Velten J** (2006) An *in vivo*, luciferase-based, Agrobacterium-infiltration assay system: implications for post-transcriptional gene silencing. *Planta* **224**: 582–597

**Ceulemans E, Ibrahim HMM, De Coninck B, Goossens A** (2021) Pathogen effectors: exploiting the promiscuity of plant signaling hubs. *Trends Plant Sci* **26**: 780–795

**Chakrabarty R, Banerjee R, Chung SM, Farman M, Citovsky V, Hogenhout SA, Tzfira T, Goodin M** (2007) pSITES vectors for stable integration or transient expression of autofluorescent protein fusions in plants: probing *Nicotiana Benthamiana*-virus interactions. *Mol Plant Microbe Interact* **20**: 740–750

**Chen H, Zou Y, Shang Y, Lin H, Wang Y, Cai R, Tang X, Zhou J** (2008) Firefly luciferase complementation imaging assay for protein-protein interactions in plants. *Plant Physiol* **146**: 368–376

**Couto D, Zipfel C** (2016) Regulation of pattern recognition receptor signalling in plants. *Nat Rev Immunol* **16**: 537–552

**Curtis MD, Grossniklaus U** (2003) A gateway cloning vector set for high-throughput functional analysis of genes in *planta*. *Plant Physiol* **133**: 462–469

**Danisman S, van Dijk AD, Bimbo A, van der Wal F, Hennig L, de Folter S, Angenent GC, Immink RG** (2013) Analysis of functional redundancies within the *Arabidopsis* TCP transcription factor family. *J Exp Bot* **64**: 5673–5685

**Davière JM, Wild M, Regnault T, Baumberger N, Eisler H, Genschik P, Achard P** (2014) Class I TCP-DELLA interactions in inflorescence shoot apex determine plant height. *Curr Biol* **24**: 1923–1928

**Dietz KJ, Vogel MO, Viehhauser A** (2010) AP2/EREBP transcription factors are part of gene regulatory networks and integrate metabolic, hormonal and environmental signals in stress acclimation and retrograde signalling. *Protoplasma* **245**: 3–14

**Falcon S, Gentleman R** (2007) Using GOSTats to test gene lists for GO term association. *Bioinformatics* **23**: 257–258

**Ferrero V, Viola IL, Ariel FD, Gonzalez DH** (2019) Class I TCP transcription factors target the gibberellin biosynthesis gene GA20ox1 and the growth-promoting genes HBI1 and PRE6 during thermomorphogenic growth in *Arabidopsis*. *Plant Cell Physiol* **60**: 1633–1645

**Gastaldi V, Lucero LE, Ferrero LV, Ariel FD, Gonzalez DH** (2020) Class-I TCP transcription factors activate the SAUR63 gene subfamily in gibberellin-dependent stamen filament elongation. *Plant Physiol* **182**: 2096–2110

**González-Fuente M, Carrère S, Monachello D, Marsella BG, Cazalé AC, Zischek C, Mitra RM, Rezé N, Cottret L, Mukhtar MS, et al.** (2020) EffectorK, a comprehensive resource to mine for *Ralstonia*, *Xanthomonas*, and other published effector interactors in the *Arabidopsis* proteome. *Mol Plant Pathol* **21**: 1257–1270

**Gonzalez-Grandio E, Pajoro A, Franco-Zorrilla JM, Tarazon C, Immink RG, Cubas P** (2017) Abscisic acid signaling is controlled by a BRANCHED1/HD-ZIP I cascade in *Arabidopsis* axillary buds. *Proc Natl Acad Sci USA* **114**: E245–e254

**Guo Z, Fujioka S, Blancaflor EB, Miao S, Gou X, Li J** (2010) TCP1 modulates brassinosteroid biosynthesis by regulating the expression of the key biosynthetic gene DWARF4 in *Arabidopsis thaliana*. *Plant Cell* **22**: 1161–1173

**Halane MK, Kim SH, Spears BJ, Garner CM, Rogan CJ, Okafor EC, Su J, Bhattacharjee S, Gassmann W** (2018) The bacterial type III-secreted protein AvrRps4 is a bipartite effector. *PLoS Pathog* **14**: e1006984

**Heese A, Hann DR, Gimenez-Ibanez S, Jones AM, He K, Li J, Schroeder JI, Peck SC, Rathjen JP** (2007) The receptor-like kinase SERK3/BAK1 is a central regulator of innate immunity in plants. *Proc Natl Acad Sci USA* **104**: 12217–12222

**Heyndrickx KS, Van de Velde J, Wang C, Weigel D, Vandepoele K** (2014) A functional and evolutionary perspective on transcription factor binding in *Arabidopsis thaliana*. *Plant Cell* **26**: 3894–3910

**Kang S, Yang F, Li L, Chen H, Chen S, Zhang J** (2015) The Arabidopsis transcription factor BRASSINOSTEROID INSENSITIVE1-ETHYL METHANESULFONATE-SUPPRESSOR1 is a direct substrate of MITOGEN-ACTIVATED PROTEIN KINASE6 and regulates immunity. *Plant Physiol* **167**: 1076–1086

**Khan M, Rozhon W, Unterholzner SJ, Chen T, Eremina M, Wurzinger B, Bachmair A, Teige M, Sieberer T, Isono E, et al.** (2014) Interplay between phosphorylation and SUMOylation events determines CESTA protein fate in brassinosteroid signalling. *Nat Commun* **5**: 4687

**Kim SH, Son GH, Bhattacharjee S, Kim HJ, Nam JC, Nguyen PD, Hong JC, Gassmann W** (2014) The *Arabidopsis* immune adaptor SRFR1 interacts with TCP transcription factors that redundantly contribute to effector-triggered immunity. *Plant J* **78**: 978–989

**Kim TW, Guan S, Sun Y, Deng Z, Tang W, Shang JX, Burlingame AL, Wang ZY** (2009) Brassinosteroid signal transduction from cell-surface receptor kinases to nuclear transcription factors. *Nat Cell Biol* **11**: 1254–1260

**Kong X, Zhang C, Zheng H, Sun M, Zhang F, Zhang M, Cui F, Lv D, Liu L, Guo S, et al.** (2020) Antagonistic interaction between auxin and SA signalling pathways regulates bacterial infection through lateral root in *Arabidopsis*. *Cell Rep* **32**: 108060

**Li M, Chen H, Chen J, Chang M, Palmer IA, Gassmann W, Liu F, Fu ZQ** (2018) TCP transcription factors interact with NPR1 and contribute redundantly to systemic acquired resistance. *Front Plant Sci* **9**: 1153

**Li S** (2015) The *Arabidopsis thaliana* TCP transcription factors: a broadening horizon beyond development. *Plant Signal Behav* **10**: e1044192

**Lin W, Lu D, Gao X, Jiang S, Ma X, Wang Z, Mengiste T, He P, Shan L** (2013) Inverse modulation of plant immune and brassinosteroid signaling pathways by the receptor-like cytoplasmic BIK1. *Proc Natl Acad Sci USA* **110**: 12114–12119

**Lopez JA, Sun Y, Blair PB, Mukhtar MS** (2015) TCP three-way handshake: linking developmental processes with plant immunity. *Trends Plant Sci* **20**: 238–245

**Lozano-Duran R, Macho AP, Boutrrot F, Segonzac C, Somssich IE, Zipfel C** (2013) The transcriptional regulator BZR1 mediates trade-off between plant innate immunity and growth. *eLife* **2**: e00983

**Lucero LE, Uberti-Manassero NG, Arce AL, Colombatti F, Alemano SG, Gonzalez DH** (2015) TCP15 modulates cytokinin and auxin responses during gynoecium development in *Arabidopsis*. *Plant J* **84**: 267–282

**Ma KW, Ma W** (2016) Phytohormone pathways as targets of pathogens to facilitate infection. *Plant Mol Biol* **91**: 713–725

**Macho AP, Zipfel C** (2014) Plant PRRs and the activation of innate immune signaling. *Mol Cell* **54**: 263–272

**Mao G, Meng X, Liu Y, Zheng Z, Chen Z, Zhang S** (2011) Phosphorylation of a WRKY transcription factor by two pathogen-responsive MAPKs drives phytoalexin biosynthesis in *Arabidopsis*. *Plant Cell* **23**: 1639–1653

**Martínez JA, Sinha N** (2013) Analysis of the role of *Arabidopsis* class I TCP genes AtTCP7, AtTCP8, AtTCP22, and AtTCP23 in leaf development. *Front Plant Sci* **4**: 406

**Martin-Trillo M, Cubas P** (2010) TCP genes: a family snapshot ten years later. *Trends Plant Sci* **15**: 31–39

**Mazur MJ, Spears BJ, Djajasaputra A, van der Graaf M, Vlachakis G, Beerens B, Gassmann W, van den Burg HA** (2017) *Arabidopsis* TCP transcription factors interact with the SUMO conjugating machinery in nuclear foci. *Front Plant Sci* **8**: 2043

**McClerkin SA, Lee SG, Harper CP, Nwumeh R, Jez JM, Kunkel BN** (2018) Indole-3-acetaldehyde dehydrogenase-dependent auxin synthesis contributes to virulence of *Pseudomonas syringae* strain DC3000. *PLoS Pathog* **14**: e1006811

**McInturf SA, Khan MA, Gokul A, Castro-Guerrero NA, Höhner R, Li J, Marjault HB, Fichman Y, Kunz HH, Goggin FL, et al.** (2022) Cadmium interference with iron sensing reveals transcriptional programs sensitive and insensitive to reactive oxygen species. *J Exp Bot* **73**: 324–338

**Mukhopadhyay P, Tyagi AK** (2015) OsTCP19 influences developmental and abiotic stress signaling by modulating ABI4-mediated pathways. *Sci Rep* **5**: 9998

**Nicolas M, Cubas P** (2016) TCP factors: new kids on the signaling block. *Curr Opin Plant Biol* **33**: 33–41

**Ning Y, Liu W, Wang GL** (2017) Balancing immunity and yield in crop plants. *Trends Plant Sci* **22**: 1069–1079

**Oh E, Zhu JY, Wang ZY** (2012) Interaction between BZR1 and PIF4 integrates brassinosteroid and environmental responses. *Nat Cell Biol* **14**: 802–809

**O’Malley RC, Huang SC, Song L, Lewsey MG, Bartlett A, Nery JR, Galli M, Gallavotti A, Ecker JR** (2016) Cistrome and epicistrome features shape the regulatory DNA landscape. *Cell* **166**: 1598

**Perez M, Guerrigue Y, Ranty B, Pouzet C, Jauneau A, Robe E, Mazars C, Galaud JP, Aldon D** (2019) Specific TCP transcription factors interact with and stabilize PRR2 within different nuclear sub-domains. *Plant Sci* **287**: 110197

**Perrella G, Davidson MLH, O’Donnell L, Nastase AM, Herzyk P, Breton G, Pruneda-Paz JL, Kay SA, Chory J, Kaiserli E** (2018) ZINC-FINGER interactions mediate transcriptional regulation of hypocotyl growth in *Arabidopsis*. *Proc Natl Acad Sci USA* **115**: E4503–e4511

**Pireyre M, Burow M** (2015) Regulation of MYB and bHLH transcription factors: a glance at the protein level. *Mol Plant* **8**: 378–388

**Poppenberger B, Rozhon W, Khan M, Husar S, Adam G, Luschnig C, Fujioka S, Sieberer T** (2011) CESTA, a positive regulator of brassinosteroid biosynthesis. *EMBO J* **30**: 1149–1161

**Powers SK, Holehouse AS, Korasick DA, Schreiber KH, Clark NM, Jing H, Emenecker R, Han S, Tycksen E, Hwang I, et al.** (2019) Nucleo-cytoplasmic partitioning of ARF proteins controls auxin responses in *Arabidopsis thaliana*. *Mol Cell* **76**: 177–190.e5

**Schommer C, Palatnik JF, Aggarwal P, Chetelat A, Cubas P, Farmer EE, Nath U, Weigel D** (2008) Control of jasmonate biosynthesis and senescence by miR319 targets. *PLoS Biol* **6**: e230

**Shigenaga AM, Berens ML, Tsuda K, Argueso CT** (2017) Towards engineering of hormonal crosstalk in plant immunity. *Curr Opin Plant Biol* **38**: 164–172

**Smith JM, Leslie ME, Robinson SJ, Korasick DA, Zhang T, Backues SK, Cornish PV, Koo AJ, Bednarek SY, Heese A** (2014) Loss of *Arabidopsis thaliana* Dynamin-Related Protein 2B Reveals Separation of Innate Immune Signaling Pathways. *PLoS Pathog* **10**: e1004578

**Spears BJ, Howton TC, Gao F, Garner CM, Mukhtar MS, Gassmann W** (2019) Direct regulation of the EFR-dependent immune response by *Arabidopsis* TCP transcription factors. *Mol Plant Microbe Interact* **32**: 540–549

**Steiner E, Efroni I, Gopalraj M, Saathoff K, Tseng TS, Kieffer M, Eshed Y, Olszewski N, Weiss D** (2012) The *Arabidopsis* O-linked N-acetylglucosamine transferase SPINDLY interacts with class I TCPs to facilitate cytokinin responses in leaves and flowers. *Plant Cell* **24**: 96–108

**Sugio A, Kingdom HN, MacLean AM, Grieve VM, Hogenhout SA** (2011) Phytoplasma protein effector SAP11 enhances insect vector reproduction by manipulating plant development and defense hormone biosynthesis. *Proc Natl Acad Sci USA* **108**: E1254–E1263

**Sun Y, Fan XY, Cao DM, Tang W, He K, Zhu JY, He JX, Bai MY, Zhu S, Oh E, et al.** (2010) Integration of brassinosteroid signal transduction with the transcription network for plant growth regulation in *Arabidopsis*. *Dev Cell* **19**: 765–777

**Valsecchi I, Guittard-Crilat E, Maldiney R, Habricot Y, Lignon S, Lebrun R, Miginiac E, Ruellan E, Jeannette E, Lebreton S** (2013) The intrinsically disordered C-terminal region of *Arabidopsis thaliana* TCP8 transcription factor acts both as a transactivation and self-assembly domain. *Mol Biosyst* **9**: 2282–2295

**Wang X, Gao J, Zhu Z, Dong X, Ren G, Zhou X, Kuai B** (2015) TCP transcription factors are critical for the coordinated regulation of ISOCHORISMATE SYNTHASE 1 expression in *Arabidopsis thaliana*. *Plant J* **82**: 151–162

**van Wersch R, Li X, Zhang Y** (2016) Mighty dwarfs: *Arabidopsis* autoimmunity mutants and their usages in genetic dissection of plant immunity. *Front Plant Sci* **7**: 1717

**Weßling R, Epple P, Altmann S, He Y, Yang L, Henz SR, McDonald N, Wiley K, Bader KC, Glasser C, et al.** (2014) Convergent targeting of a common host protein-network by pathogen effectors from three kingdoms of life. *Cell Host Microbe* **16**: 364–375

**Xiao YL, Smith SR, Ishmael N, Redman JC, Kumar N, Monaghan EL, Ayele M, Haas BJ, Wu HC, Town CD** (2005) Analysis of the cDNAs of hypothetical genes on *Arabidopsis* chromosome 2 reveals numerous transcript variants. *Plant Physiol* **139**: 1323–1337

**Xu SL, Chalkley RJ, Maynard JC, Wang W, Ni W, Jiang X, Shin K, Cheng L, Savage D, Huhmer AF, et al.** (2017) Proteomic analysis reveals O-GlcNAc modification on proteins with key regulatory functions in *Arabidopsis*. *Proc Natl Acad Sci USA* **114**: E1536–e1543

**Yang L, Teixeira PJ, Biswas S, Finkel OM, He Y, Salas-Gonzalez I, English ME, Epple P, Mieczkowski P, Dangl JL** (2017) *Pseudomonas syringae* type III effector HopBB1 promotes host transcriptional repressor degradation to regulate phytohormone responses and virulence. *Cell Host Microbe* **21**: 156–168

**Yin Y, Vafeados D, Tao Y, Yoshida S, Asami T, Chory J** (2005) A new class of transcription factors mediates brassinosteroid-regulated gene expression in *Arabidopsis*. *Cell* **120**: 249–259

**Yin Y, Wang ZY, Mora-Garcia S, Li J, Yoshida S, Asami T, Chory J** (2002) BES1 accumulates in the nucleus in response to brassinosteroids to regulate gene expression and promote stem elongation. *Cell* **109**: 181–191

**Yu X, Li L, Zola J, Aluru M, Ye H, Foudree A, Guo H, Anderson S, Aluru S, Liu P, et al.** (2011) A brassinosteroid transcriptional network revealed by genome-wide identification of BES1 target genes in *Arabidopsis thaliana*. *Plant J* **65**: 634–646

**Zavaliev R, Mohan R, Chen T, Dong X** (2020) Formation of NPR1 condensates promotes cell survival during the plant immune response. *Cell* **182**: 1093–1108.e18

**Zhang N, Wang Z, Bao Z, Yang L, Wu D, Shu X, Hua J** (2018) MOS1 functions closely with TCP transcription factors to modulate immunity and cell cycle in *Arabidopsis*. *Plant J* **93**: 66–78

**Zhang Y, Mayba O, Pfeiffer A, Shi H, Tepperman JM, Speed TP, Quail PH** (2013) A quartet of PIF bHLH factors provides a transcriptionally centered signaling hub that regulates seedling morphogenesis through differential expression-patterning of shared target genes in *Arabidopsis*. *PLoS Genet* **9**: e1003244

**Zhou J, Wu S, Chen X, Liu C, Sheen J, Shan L, He P** (2014) The *Pseudomonas syringae* effector HopF2 suppresses *Arabidopsis* immunity by targeting BAK1. *Plant J* **77**: 235–245

**Zhou Y, Xun Q, Zhang D, Lv M, Ou Y, Li J** (2019) TCP transcription factors associate with PHYTOCHROME INTERACTING FACTOR 4 and CRYPTOCHROME 1 to regulate thermomorphogenesis in *Arabidopsis thaliana*. *iScience* **15**: 600–610

**Zhou Y, Zhang D, An J, Yin H, Fang S, Chu J, Zhao Y, Li J** (2018) TCP transcription factors regulate shade avoidance via directly mediating the expression of both PHYTOCHROME INTERACTING FACTORS and auxin biosynthetic genes. *Plant Physiol* **176**: 1850–1861

**Zhu P, Lister C, Dean C** (2021) Cold-induced *Arabidopsis* FRIGIDA nuclear condensates for FLC repression. *Nature* **599**: 657–661

**Zipfel C, Kunze G, Chinchilla D, Caniard A, Jones JD, Boller T, Felix G** (2006) Perception of the bacterial PAMP EF-Tu by the receptor EFR restricts Agrobacterium-mediated transformation. *Cell* **125**: 749–760